Tech Science Press

Detection of Lung Tumor Using ASPP-Unet with Whale Optimization Algorithm

**Mimouna Abdullah Alkhonaini[1], Siwar Ben Haj Hassine[2], Marwa Obayya[3], Fahd N. Al-Wesabi[2],
Anwer Mustafa Hilal[4,*], Manar Ahmed Hamza[4], Abdelwahed Motwakel[4] and Mesfer Al Duhayyim[5]**

[1]Department of Computer Science, College of Computer and Information Sciences, Prince Sultan University, 11564,
Saudi Arabia
[2]Department of Computer Science, College of Science and Arts, King Khalid University, Mahayil, Asir, 61913,
Saudi Arabia
[3]Department of Biomedical Engineering, College of Engineering, Princess Nourah Bint Abdulrahman University,
Riyadh, 11671, Saudi Arabia
[4]Department of Computer and Self Development, Preparatory Year Deanship, Prince Sattam bin Abdulaziz University,
AlKharj, 16278, Saudi Arabia
[5]Department of Natural and Applied Sciences, College of Community-Aflaj, Prince Sattam bin Abdulaziz University,
16278, Saudi Arabia
*Corresponding Author: Anwer Mustafa Hilal. Email: a.hilal@psau.edu.sa

Abstract: The unstructured growth of abnormal cells in the lung tissue creates tumor. The early detection of lung tumor helps the patients avoiding the death rate and gives better treatment. Various medical image modalities can help the physicians in the diagnosis of disease. Many research works have been proposed for the early detection of lung tumor. High computation time and misidentification of tumor are the prevailing issues. In order to overcome these issues, this paper has proposed a hybrid classifier of Atrous Spatial Pyramid Pooling (ASPP)-Unet architecture with Whale Optimization Algorithm (ASPP-Unet -WOA). To get a fine tuning detection of tumor in the Computed Tomography (CT) of lung image, this model needs pre-processing using Gabor filter. Secondly, feature segmentation is done using Guaranteed Convergence Particle Swarm Optimization. Thirdly, feature selection is done using Binary Grasshopper Optimization Algorithm. This proposed (ASPP-Unet -WOA) is implemented in the dataset of National Cancer Institute (NCI) Lung Cancer Database Consortium. Various performance metric measures are evaluated and compared to the existing classifiers. The accuracy of Deep Convolutional Neural Network (DCNN) is 93.45%, Convolutional Neural Network (CNN) is 91.67%, UNet obtains 95.75% and ASPP-UNet-WOA obtains 98.68%. compared to the other techniques.

1 Introduction

In the medical diagnostics, digital image processing plays a vital role [1]. Biomedical image processing is used to process the digital image in the field of biomedical science [2]. For the diagnosis of disease at the early stage, bio-medical field needs an accurate detection using computing intelligent approach [3]. It could provide more precise and active treatment for the disease. There are various medical image modalities like Magnetic Resonance Imaging (MRI), ultrasound, Computed Tomography (CT) scanners that are used in the diagnosis of image in a greater way. CT is the most effective approach of lung tumor detection and tumor pathology [4].

The analysis of tumor is a tedious and time consumption task. CT plays a vital role and more sensitive in the determination of tumor size. Computer Aided Diagnosis (CAD) has been used for the early prediction of lung cancer [5]. As far as CAD model is concerned, sensitivity, specificity, cost effectiveness and accuracy are achieved in the analysis of lung cancer [6]. For enhancing the affected region of the disease, CAD uses the digital images [7]. The prediction of diseases is done through the information gathered from the image modalities and as well as the clinical analysis is carried out by the radiologist for the final decision [8].

The use of multimodal medical images will lead the physician to take more time to diagnosis and provides a better treatment. Therefore, in order to get an accurate and an effective treatment, the bio-medical field needs an automatic segmentation of tumor which relieves the physicians by increasing the consistency and efficiency [9–11].

The issues in the existing techniques have high consumption of energy, inaccurate detection, and high time complexity. To overcome these problems, the proposed work gives more accurate detection of tumor in the lung and similarly, it detects the tumor at the earlier stage in an effective manner.

The contributions of the proposed work are:

1. To implement an enhanced version of feature selection by applying binary grasshopper optimization algorithm.
2. Proposed work (ASPP-UNet-WOA) is applied for the detection of tumor in the lung image by optimizing the features subset.

The rest of the research article is written as follows: Section 2 discusses the related work on various classification techniques of lung tumor image processing and methods. Section 3 shows the algorithm process and general working methodology of proposed work. Section 4 evaluates the implementation and results of the proposed method. Section 5 concludes the work and discusses the result evaluation.

2 Related Work

The abnormal growth of cells in the lung tissue is considered as tumor. Early detection and prevention of high risk in the treatment of the disease are the essential things. In medical image diagnosis of disease, the accuracy and consistency are very important things for the survival of human beings. In the training of CT lung image data set, Feed Forward Neural Network (FFNN), Feed Forward Back Propagation (FWBP) were used. For providing better classification of tumor, Feed Forward Back Propagation (FWBP) was applied [12].

It is difficult to diagnosis using CNN and sometimes it detects falsely. Moreover, 3D CNN has handled this type of lung pathology. In order to produce better result, it combines the max pooling layer and convolutional layer which were applied to produce each CNN. ReLU is applied here as activation function along with Softmax layer which is applied fully to connect the layer and finally it produces

the result [13]. This paper [14] proposed an automatic detection of lung tumor using public dataset of LIDC-IRDI. It uses MultiScene Deep Learning Framework which provides CT lung images as input and obtains probability distribution of distinct gray levels using threshold segmentation. Tab. 1 shows the survey on existing algorithms in the base of tumor in lung image.

Table 1: Existing algorithms in the base of tumor in lung image

Pre-processing technique	
Author name	Method
Asuntha et al. (2020) [15]	Adaptive bilateral filter
Ozdemir et al. (2019) [16]	Adaptive gaussian filtering
Vas et al. (2017) [17]	Median filtering
Teramoto et al. (2017) [18]	Gaussian and convolutional edge enhancement filtering
Segmentation of image	
Saric et al. (2019) [19]	Region of interest
Rahman et al. (2019) [20]	Otsu thresholding
Alam et al. (2018) [21]	Watershed transform
Classification of image	
Shanthi et al. (2020) [22]	Stochastic diffusion search algorithm & neural networks (SDS-NN)

3 Methodology

One of the high risky diseases is lung tumor. But early prediction can save the life of a patient. But it is undeniable that the prediction of tumor is a challenging task. This proposed work consists of following phases: pre-processing, segmentation, extraction of the feature, feature selection, and classifying of tumor from the CT lung image. These phases are shown in Fig. 1.

Fig. 1 shows the two phases namely, training phase and testing phase. In the segmentation phase, using Guaranteed Convergence Particle Swarm Optimization Algorithm is applied in the filtered input lung tumor image (GCPSOA). The feature extraction is done using GLCM and in the feature selection, binary grasshopper optimization algorithm (BGOA) is used. From the selected features, tumor lung image is classified using Atrous Spatial Pyramid Pooling (ASPP)-Unet architecture with whale optimization algorithm (ASPP-Unet -WOA).

3.1 Pre-processing

Pre-processing is the most significant step in the detection of lung tumor. To enhance the accuracy in the detection of tumor, removal of unnecessary signals in the image pre-processing are needed. In this work Gabor filter is used to remove the noise in the lung tumor image.
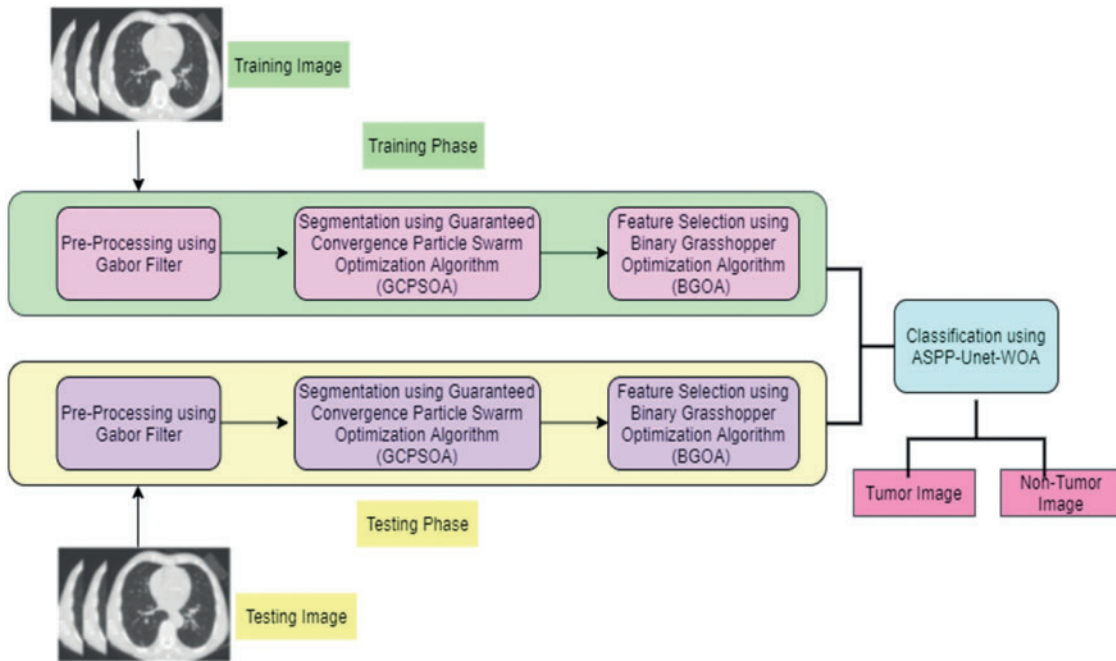
Figure 1: Architecture of proposed work

3.1.1 Gabor Filter

Gabor is a multi-scale, multi resolution filter [23,24]. Gabor filter can be applied in four different orientations and five different frequency values. The steps involved in Gabor filter using Gaussian rule can be referred in the article [25].

Apply the Gaussian function of standard deviation to the lung tumor image (img)_(i, j) with different angles like 0°, 20°, 40°, 60°, 120° and various orientations such as 60, 80,120 and 140 using Eq. (1).

$$img\,(i,j,\sigma) = e^{-\frac{(i-i_0)^2}{2\sigma_i^2} - \frac{(j-j_0)^2}{2\sigma_j^2}}\,e^{j\left(\omega_{i0}i + \omega_{j0}j\right)} \tag{1}$$

where,

ω_{i0}, ω_{j0}-Centre frequency of i and j directions of image.

σ_i, σ_j-Standard deviation of the Gaussian function with i and j axis or direction.

i, j-Position of the image in pixel format.

Step 4: Substitute the Eq. (1) in Eq. (2).

$$\varphi\,(i,j,\omega,\sigma,\,\theta) = e^{-\frac{(i\cos\theta_k - j\sin\theta_k)^2}{2\sigma_i^2} + \frac{(-i\sin\theta_k - j\cos\theta_k)^2}{2\sigma_j^2}}\,e^{xj\left(\omega_{i0}i\cos\theta_k + \omega_{j0}j\sin\theta_k\right)} \tag{2}$$

$$i\theta_k = i\cos(\theta_k) + j\sin(\theta_k) \tag{3}$$

$$j\theta_k = i\sin(\theta_k) + j\sin(\theta_k)\ . \tag{4}$$

3.1.2 Data Augmentation

To get better quality of classification, data augmentation process is done in the Lung image. It involves transformation of CT lung image performing rotation at 90 degrees and flipping the image horizontal operation [26–29].

3.1.3 Normalization of the Image Using Min-Max Normalization Technique

To normalize the input CT lung image of size 512×512 pixels and the value of intensity between [0, 1] is evaluated in Eq. (5)

$$p_i = \frac{(q_i - \min(q))}{(\max(q) - \min(q))} \tag{5}$$

Here, p_i is the normalized intensity value of position of image q_i $(1 = 1, 2, \ldots, n)$ and intensity values of maximum and minimum are represented as $max(q)$ and $min(q)$. After applying the normalization, the size of image gets resized to 256×256 pixels [30,31].

3.2 Segmentation of Lung Tumor Image

Segmentation is a process of dividing the filtered lung tumor image into sub-regions. To detect the tumor easily, segmentation process is applied. In this work, Guaranteed Convergence Particle Swarm Optimization Algorithm is applied (GCPSOA). Let assume that population of the swarm is *max* particles in the dimensional space of *D*. Then the optimal position of jth particle is represented as pos_i, $i = 1, 2, \ldots, max$. Refer Eqs. (6) and (7).

$$vel_{i,D}(it+1) = \omega.vel_{i,D}(it) + coef_1.rnd_1.\left(pbest_{i,D}(it) - x_{i,D}(it)\right) + coef_2.rnd_2.\left(sgbest_{j,D}(it) - x_{i,D}(it)\right) \tag{6}$$

$$x_{i,D}(it+1) = x_{i,D}(it) + vel_{i,D}(it+1) \tag{7}$$

where, *it* shows iteration number and dimension *D*. $x_{i,D}(it)$ is D^{th} dimension variable of the ith particle in the iteration. $vel_{i,D}$ is the velocity for particle $pbest_{i,D}(it)$ in the dimension variable. The global best position of swarm population is represented as $sgbest_{j,D}(it)$.$coef_1$ and $coef_2$ coefficient variables with random vectors like rnd_1 and rnd_2 and the diameter of search area ρ are uniformly distributed in the interval of [0,1]. The fitness function of particle swarm optimization algorithm is defined in Eq. (8)

$$maximize\ fn = \sum_{i=1}^{n} \frac{inter\_cluster\ distance}{intra\_cluster\ distance} \tag{8}$$

The convergence of particles is determined by implementing the Eqs. (6) and (7). Then transformed into the dynamic form as described in Eq. (9).

$$\begin{bmatrix} vel(it+1) \\ x(it+1) \end{bmatrix} = \begin{bmatrix} \omega & -\varphi(it) \\ \omega & 1-\varphi(it) \end{bmatrix} \begin{bmatrix} vel(t) \\ x(t) \end{bmatrix} + \begin{bmatrix} \varphi_1(it) & \varphi_2(it) \\ \varphi_1(it) & \varphi_2(it) \end{bmatrix} \begin{bmatrix} pbest_i(it) \\ sgbest_j(it) \end{bmatrix} \tag{9}$$

where, $\varphi_1 = coef_1.rnd_1$, $\varphi_2 = coef_2.rnd_2$ and $\varphi = \varphi_1 + \varphi_2$. The optimal position pos_i of the particle and finally it converges at the position of swarm's population $spop_j$. The diameter search area can be updated as given in Eq. (10).

$$\rho(it+1) = \begin{cases} 2\rho(it), & num\_successes > suc \\ \left(\frac{1}{1.5}\right)\rho(it), & num\_failures > fac, \\ \rho(it), & otherwise \end{cases} \tag{10}$$

where, num_successes and num_failures are represented as number of successes and failures, suc and fac are defined as threshold parameter values.

3.3 Feature Selection

In order to get fine tuning classification of image, feature selection task is required by which reducing the features quantity by means of removing redundant and irrelevant information is possible. In this work, Binary Grasshopper Optimization Algorithm (BGOA) is implemented. Grasshoppers are treated as a pest. The key feature of these pests is connected to their movements. At their larval state, it has a slow movement when compared to its adult state. Since at the adult state, its movement is rapid. The movement of the grasshoppers can be represented as in Eq. (11).

$$A_i^d = c \left(\sum_{j=1, j \neq i}^{N} c \frac{upb_d - lwb_d}{2} s \left(\left| A_j^d - A_i^d \right| \right) \frac{A_j - A_i}{d_{ij}} \right) + T_d \tag{11}$$

where, upb_d is upper bound in the dth dimension, lwb_d is lower bound in the dth dimension. T_d is the target value of dth dimension, c is the value of coefficient which reduces the proportional value of the comfort zone to the iterations and it is evaluated as per Eq. (12).

$$c = c_{max} - iter \frac{c_{max} - c_{min}}{L} \tag{12}$$

Here, *iter* is the current iteration. L is the total number of iterations, c_{max} is the maximum coefficient value of 1, c_{min} is the minimum coefficient value of 0.00001. This binarization value of continuous space transforms into 0 or 1. For this binary transformation, it needs Transfer Function (TF). Now the Eq. (11) has changed into Eq. (13) as given below:

$$\Delta A = c \left(\sum_{j=1, j \neq i}^{N} c \frac{upb_d - lwb_d}{2} s \left(\left| A_j^d - A_i^d \right| \right) \frac{A_j - A_i}{d_{ij}} \right) \tag{13}$$

Transfer Function (TF) has two types of functions based on their shapes such as Sigmoidal (S-shaped) and Hyperbolic tan (V-shaped). The Sigmoidal (S-shaped) function is represented in Eq. (14)

$$T (\Delta A_i) = \frac{1}{1 + e^{-\Delta A_i}} \tag{14}$$

where ΔA indicates the velocity of search agent at i^{th} repetition. Now the current location of the grasshopper is based on the probability value which is given in Eq. (15):

$$A_{t+1}^d = \begin{cases} 1 & if \ rnd_1 < T \left(\Delta A_{t+1}^d \right) \\ 0 & if \ rnd_1 \geq T \left(\Delta A_{t+1}^d \right) \end{cases} \tag{15}$$

where the dth dimension of the grasshopper is denoted as A_{t+1}^d, and rnd_1 is a random number that lies between 0 and 1.

Hyperbolic tan (V-shaped) is represented as (16)

$$T (\Delta A_i) = |\tanh (\Delta A_i)| \tag{16}$$

Then the improved version of current location grasshopper is represented in Eq. (16):

$$A_{t+1}^d = \begin{cases} -A_t^d rnd_2 \leq & T\left(\Delta A_{t+1}^d\right) \\ A_t^d rnd_2 \geq & T\left(\Delta A_{t+1}^d\right) \end{cases} \qquad (17)$$

Here rnd_2 is the random number between 0 and 1. See Eq. (17)

For every iteration, fitness function is calculated. It is carried out because the aim of the feature selection is to enhance the accuracy and decrease the number of selected features. For the best solution, the nominated features are to be selected. For these nominated features, the classification rate is also reduced. The fitness function for the selected features is defined in Eq. (18):

$$fit = \alpha \gamma_R (D) + \beta \frac{|R|}{|N|} \qquad (18)$$

where the taxonomy error rate of the classifier is represented as $\gamma_R (D)$, $|N|$ is the number of features and $|R|$ is the number of selected features and α is the taxonomy error rate, β is the length of the subset. Hence, $\alpha \in [0, 1]$ and the value of $\beta = (1 - \alpha)$. The algorithm of Binary Grasshopper Optimization Algorithm (BGOA) is discussed.

3.4 Classification Using ASPP-Unet-WOA

The selected features are provided to the ASPP-Unet (Atrous spatial pyramid pooling) architectures as the input. ASPP-Unet model is similar to the U-Net model in the aspects of contracting the path with CNN model. The architecture of ASPP-Unet model is given in the Fig. 2.
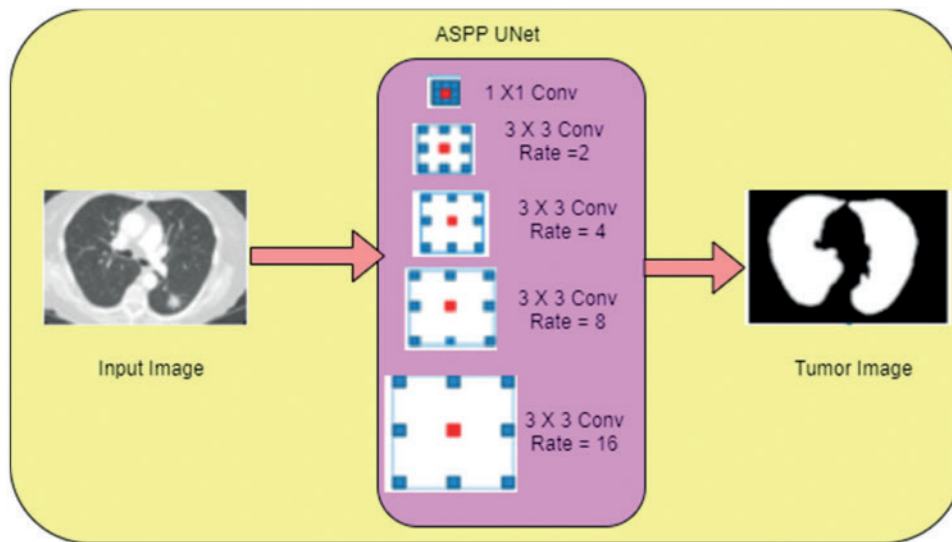

Figure 2: Architecture of ASPP Unet

Fig. 2 shows a pyramid-like structure and each down layer consists of two sequential unpadded 3×3 convolutions. Each convolution operation is executed by an activation function in the basis of element-wise. After the convolution execution, the feature maps get doubled. In this work Exponential

linear unit (Elu) function is applied to perform the activation function and it is given in Eq. (19):

$$af(x) = \begin{cases} x & (x > 0) \\ \alpha(exp(x) - 1) & (x < 0) \end{cases} \tag{19}$$

where α is a parameter value between 0 and 1. To reduce the resolution of feature maps, 2×2 max pooling operation is applied in the contracting path between the lower and the upper layers. The size of the feature maps gets reduced to $1/8^{th}$ of its original image in the bottom layer with 3×3 convolution at the rate of 1, 2, 4, 8, 16 which is implemented parallelly. The objective function of fitness in each iteration is given in Eqs. (20) and (21)

$$fit_{obj} = E * (1 + \beta) / RF \tag{20}$$

$$RF = m/S \tag{21}$$

where β is the constant value of 0.5, E is the overall error rate, m is the number of selected features, and S is the number of swarms. Hunting of prey with the help of searching agent (best) and chasing of prey are the behaviours of whale, and due to that the position gets changed in an encircled way. This can be defined in Eqs. (22) and (23):

$$\vec{F} = \left| \vec{C} \cdot \vec{Y} * (j) - \vec{Y}(j) \right| \tag{22}$$

$$\vec{Y}(j+1) = \vec{Y}^*(j) - P \cdot \vec{F} \tag{23}$$

where, C and P are the coefficient vector values, j is the iteration. $\vec{Y}$ represents the position of vector value, Y^* denotes the best solution of position vector. These coefficient vector values are shown in the Eqs. (24) and (25).

$$P = 2e.rnd - e \tag{24}$$

$$L = 2.rnd \tag{25}$$

e is the linear decreasing value from 3 to 0 and *rnd* is the random vector value $[-1, 1]$. In the formulation of bubble net phase for the search of prey and the updating position of spiral process are defined in Eq. (26)

$$\vec{Y}(j+1) = F' . e^{bh} . \cos(2\pi h) + \vec{Y} * (j) \tag{26}$$

The humpback whales chase around the prey within the spiral-shaped and the shrinking circle simultaneously to catch the prey. The algorithm of the proposed work using ASPP-Unet-WOA is given below:

Algorithm 1: Classification using ASPP-Unet-WOA

Input: Selected features of image, Atrous CNN layer and train the data set
Output: Optimized solution in classify the tumor in the lung image
Step 1: Initialize the population of WOA algorithm
Step 2: Calculate the objective fitness function using Eq. (20)
Step 3: While (j < max-iterations)
Step 4: For each search agent

                                                                                                                    (Continued)

Algorithm 1: Continued

Step 5: Construct ASPP-Unet with WOA
Step 6: Update e, p, l and m
Step 7: If (m < 0.5)
Step 8: If (|P| < 2)
Step 9: Change the current position of search agent using Eq. (22)
Step 10: Else If (|P| > 2)
Step 11: Randomly choose the search agent
Step 12: Search to find the global best position of search agent.
Step 13: End if
Step 14: Else if (m > 0.5)
Step 15: Update the position of current search agent using Eq. (26)
Step 16: By using Eqs. (24) and (25) replace the new best position globally.
Step 17: End if
Step 18: Update the best solution in the search agent
Step 19: j = j + 1
Step 20: End While
Step 21: Return the best position of the search agent

4 Result and Analysis

4.1 Dataset Description

For the early detection of lung tumor, this work has implemented using 150 samples of lung CT images. The images are obtained from the NCI Lung Cancer Database Consortium. Computed Tomography (CT) scan images are used in this study in order to detect the tumor in the lung image in an effective and accurate way.

The statistical performance of metric measures are given below:

Accuracy

It is used to evaluate the classification of correct lung tumor images accurately. See Eq. (27).

$$accuracy = \frac{TP + TN}{TP + TN + FP + FN} X100 \qquad (27)$$

Sensitivity

It is used in the evaluation of sensitivity to measure how far the lung tumor images are identified. See Eq. (28).

$$Sensitivity = \frac{TP}{TP + FN} X100 \qquad (28)$$

Specificity

It is used to evaluate the rate between True Negative (TN) and True Positive (TP). See Eq. (29).

$$Specificty = \frac{TN}{TN + FP} X100 \qquad (29)$$

Dice Similarity Coefficient

It is used to evaluate the ratio between tumor lung images and non-tumor lung images. See Eq. (30)

$$DSC = \frac{2TP}{FP + 2TP + FN} X100 \tag{30}$$

Precision

See Eq. (31).

$$precision = \frac{TP}{TP + FP} X100 \tag{31}$$

Recall

See Eq. (32).

$$recall = \frac{TP}{TP + FN} \tag{32}$$

JACCARD Similarity Index (JSI)

It is used to evaluate the similarity between the actual tumor image pixels and the predicted tumor image pixels using Eq. (33):

$$JSI = \frac{TP}{TP + FN + FP} X100 \tag{33}$$

False Positive Rate (FPR)

It is used to evaluate the ratio between correctly identified pixels of brain image to wrongly identified pixels of brain image using Eq. (34):

$$FPR = 1 - Specificty \tag{34}$$

False Negative Rate (FNR)

It is used to evaluate the positive proportion value but negative pixel value is identified using

$$FNR = 1 - Sensitivity \tag{35}$$

Performance metric based on error rate of the Root Mean Square Error (RMSE), Signal-to-Noise-Ratio (SNR), Peak Signal-to-Noise-Ratio (PSNR), and Mean Absolute Error (MAE). The error rate value is calculated as fro Eqs. (36) to (37).

:

$$PSNR = 20\log_{10} \left(\frac{255^2}{MAE} \right) \tag{36}$$

$$MAE = \frac{1}{MN} \sum_{i=1}^{M} \sum_{j=1}^{N} |X(i,j) - Y(i,j)| \tag{37}$$

$$RMSE = \sqrt{\frac{1}{N} \sum_{i=1}^{N} \left(X_i - \widehat{X_i} \right)^2} \tag{38}$$

$$SNR(db) = 20\log \left(\frac{V_{RMS(Signal)}}{V_{RMS(Noise)}} \right) \tag{39}$$

Speckle Suppression Index Value (SSI)

$$SSI = \frac{\sqrt{Var\left(I_f\right)}}{Mean\left(I_f\right)} * \frac{Mean\left(I_o\right)}{\sqrt{Var\left(I_o\right)}} \tag{40}$$

Speckle Suppression and Mean Preservation Index (SMPI)

$$SMPI = Q * \frac{\sqrt{Var\left(I_f\right)}}{\sqrt{Var\left(I_o\right)}} \tag{41}$$

$$Q = 1 + \left|Mean\left(I_o\right) - Mean\left(I_f\right)\right| \tag{42}$$

where, I_f is the filtered image and I_o is the noisy image. This SSI tends to be less than 1 if the filter performance is efficient in reducing the speckle noise (Sheng and Xia, 1996). Tab. 2 shows SSI index value for filter image.

Table 2: SSI value for filtering lung tumor image

	SSI				
Sample images	Median filter	Adaptive median filter	Average filter	Rolling guidance filter	Gabor filter
Image 1	0.8467	0.8411	0.9734	0.8178	0.7902
Image 2	0.8321	0.8178	0.9521	0.8023	0.7812
Image 3	0.8261	0.8212	0.9267	0.8202	0.7867
Image 4	0.8292	0.8234	0.9658	0.8134	0.7843
Image 5	0.8399	0.8345	0.9489	0.8254	0.7267

Tab. 2 shows the performance of median filter, adaptive median filter, average filter, rolling guidance filter and Gabor filter with gaussian rule that are applied. Here Gabor filter shows very good performance in suppressing the noise of speckle over the other filters. Gabor filter undergoes various frequency and orientation which enhance the image for the further process. Tab. 3 shows the SMPI index value for the filtering image.

Tab. 3 shows the performance of median filter, adaptive median filter, average filter rolling guidance filter and Gabor filter with gaussian rule that are applied. Gabor filter got good performance in filtering the noise in the image as well as it enhances the contrast of the image. Fig. 3 shows the sample images after applying the filtering.

4.2 Segmentation

In the segmentation process, this work has implemented the Guaranteed Convergence Particle Swarm Optimization Algorithm (GCPSOA). This work is compared with the existing segmentation techniques of the watershed, Otsu threshold algorithm [32,33]. Moreover, GCPSO algorithm is based on the population and searching for the best solution. It uses the velocity as an impartial value of the function. Update its velocity value when the particle comes closer to the best solution. Fig. 3 shows the segmentation of the lung tumor detection output using GCPSO algorithm.

Table 3: SMPI value for filtering the lung tumor image

SMPI

Sample images	Median filter	Adaptive median filter	Average filter	Rolling guidance filter	Gabor filter
Image 1	0.9512	0.9467	0.9832	0.9178	0.9012
Image 2	0.9321	0.9287	0.9787	0.9023	0.9011
Image 3	0.9431	0.9345	0.9621	0.9202	0.9145
Image 4	0.9389	0.9265	0.9558	0.9134	0.9043
Image 5	0.9334	0.9323	0.9512	0.9254	0.9167
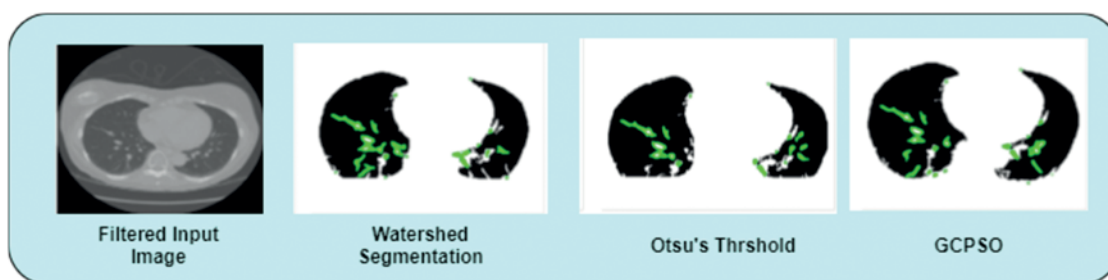
Figure 3: Segmentation

4.3 Feature Selection

This work has implemented the Binary Grasshopper Optimization Algorithm (BGOA) for feature selection of lung tumor image. Tab. 4 shows the sensitivity, specificity and precision performance comparison using various feature of selection techniques such as Particle Swarm Optimization Algorithm (PSOA), K-means Clustering (KmC) and BGOA.

Table 4: Feature selection

Feature selection

Method name	Sensitivity%	Specificity%	Precision%
PSOA	93.12	92.78	93.15
KMC	89.45	87.56	91.61
BGOA	97.89	98.12	98.81

Tab. 4 shows sensitivity, specificity and precision which provide the best performances for BGO algorithm compared to the existing algorithms. BGOA provides the optimized features selection of the lung tumor image.

Fig. 4 shows the accuracy rate of BGOA that outperforms when compared to the other existing algorithms in the selection of features from the lung tumor images.
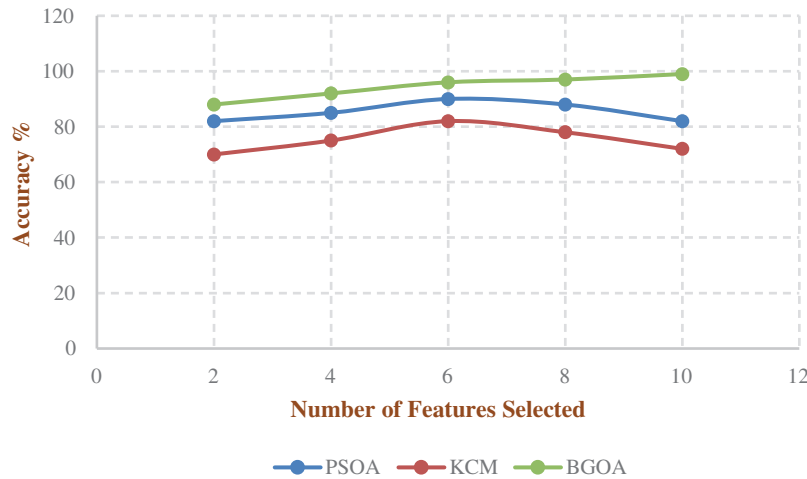
Figure 4: Accuracy rate of feature selection

4.4 Classification

The proposed ASPP-Unet-WOA technique is accurately identified from the lung tumor image. Gabor filter with Gaussian rule is used to remove the noise from the images. Using Guaranteed Convergence Particle Swarm Optimization Algorithm (GCPSOA) is used to segment the lung tumor from the pre-processed image. After segmentation, BGOA is used to select the relevant features from the CT lung image, and it enhances the classification accuracy. After feature selection process, the selected features are provided to the ASPP-Unet-WOA classifier to detect the lung tumor.

The proposed work is compared with the existing classifiers of DCNN, CNN, UNet. Tab. 4 shows the performance metric measures of DSC, FPR, FNR and JSI using Eqs. (30) to (35).

Tab. 5 shows the analysis of various metric measures that produce the best performance compared to the other existing approach. The metric measure of DSC value is highly achieved as 98.67% compared with DCNN of 88.21%, CNN of 84.78%, and UNet is 86.56%. FPR rate proposed algorithm has secured 0.0525 rate and FNR rate is 0.0041 compared to the existing model. JACCARD Similarity Index (JSI) measure has got 98.75%. Tab. 5 shows the computation time of the proposed work ASPP-UNet-WOA at various stages.

Table 5: Comparison of various metric measures

Algorithm	DSC %	FPR	FNR	JSI %
DCNN [34]	88.21	0.42	0.032	92.75
UNet [35]	86.56	0.38	0.019	94.87
ASPP-UNet-WOA (Proposed work)	98.67	0.0525	0.0041	98.75

From the Tab. 5. it is observed that the computation times on running the detection of tumor program in DCNN, CNN, UNet and ASPP-UNet-WOA approaches are provided. The robustness of ASPP-UNet-WOA performs well better in both the aspects of accuracy and the time taken for computation. Fig. 5 shows the accuracy rate of classifier model.
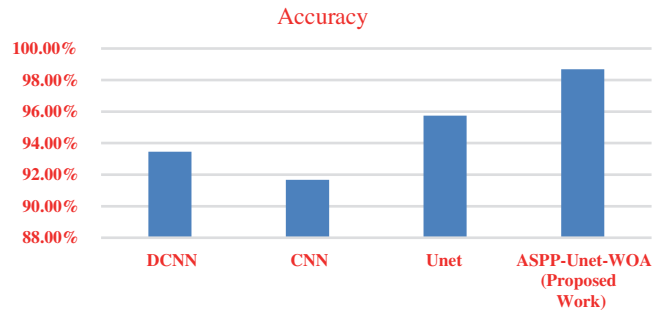
Figure 5: Accuracy

Fig. 5 shows the accuracy rate of proposed work ASPP-UNet-WOA technique Tab. 6. This proposed study outperforms with the other existing algorithms in the early detection of lung tumor. Tab. 7 shows the comparison of the proposed work with the existing scheme.

Table 6: Computation time of ASPP-UNet-WOA

Model name	Gabor filter (Sec)	GCPSOA Segmentation (Sec)	BGOA Feature selection (Sec)	ASPP-Unet-WOA Classification (Sec)	Total time (Sec)
DCNN	1.97	7.16	65.54	45.75	120.42
CNN	1.96	7.16	65.54	40.55	115.21
Unet	1.92	6.75	60.25	30.55	99.47
ASPP-Unet-WOA (Proposed Work)	1.75	6.68	59.75	20.75	88.93

Table 7: Comparison of proposed work with the existing scheme

Author name	Classifier	Data set	Accuracy (%)
Suresh [36]	DCNN	LIDC-IDRI	97.8
ASPP-Unet-WOA	ASPP-Unet-WOA	NCI LCDC	98.68

From the Tab. 7. it is observed that the proposed scheme has obtained the best accuracy for NCI LCDC dataset compared to the existing methods. The comparison performance metrics of accuracy, sensitivity, specificity, FPR, and FNR are better for the proposed method compared to the existing techniques. From these results, it is stated that the proposed ASPP-Unet-WOA method is the best selection for the early diagnosis of lung tumor.

From the Fig. 6. it is observed that PSNR value must be increased and MAE value must be decreased for the best detection of tumor image. The proposed approach gives the better error rate

value on the basis of accuracy. In the proposed work, the value of PSNR gets increased and the value of MAE gets decreased compared to the other existing techniques.
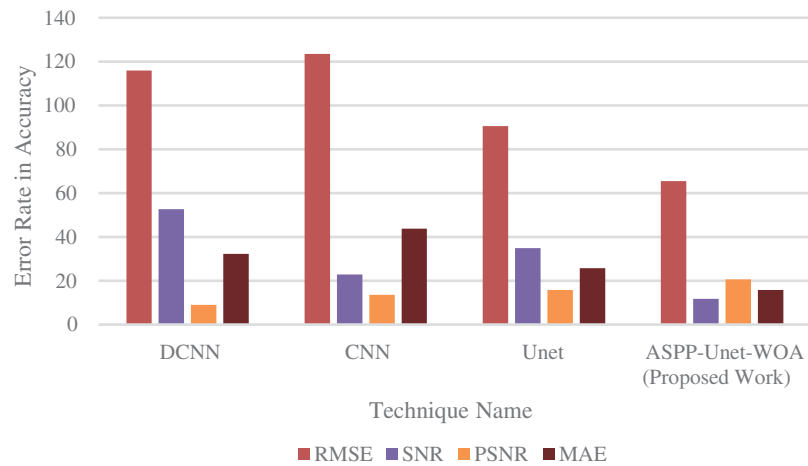

Figure 6: Error rate in accuracy

5 Conclusions

This paper presents the detection of lung tumor using ASPP-UNet with whale optimization algorithm. Diagnosis at the early stage can decrease the death rate. In this paper, ASPP-UNet-WOA has proposed various processes like pre-processing, segmentation, feature selection and classification or detection of tumor in the CT lung image. In the pre-processing stage, Gabor filter with Gaussian rule is used. Then Guaranteed Convergence Particle Swarm Optimization Algorithm (GCPSOA) is used for the segment of tumor part in the CT lung image. After the segmentation process, the relevant features are selected using BGOA technique. These optimized features are provided to the classifier of ASPP-UNet-WOA and lung tumor is effectively detected. This paper collected the dataset from NCI lung cancer database consortium. The accuracy of DCNN is 93.45%, CNN is 91.67%, UNet obtains 95.75% and ASPP-UNet-WOA obtains 98.68%. For the future studies, the proposed work can be extended to the diagnosis strategies.

Conflicts of Interest: The authors declare that they have no conflicts of interest to report regarding the present study.

References

[1]   S. N. Mazhir, A. H. Ali, F. W. Hadi and A. N. Mazher, "Studying the effect of dielectric barrier discharges on the leukemia blood cells using digital image processing," *IOSR Journal of Pharmacy & Biological Sciences*, vol. 12, no. 2, pp. 6–12, 2017.

[2]   M. P. Beham and A. Gurulakshmi, "Morphological image processing approach on the detection of tumor and cancer cells," in *Proc. Int. Conf. on Distributed Computing Systems(ICDCS)*, Coimbatore, India, pp. 350–354, 2012.

[3]   D. Gutman, N. Codella, E. Celebi, B. Helba, M. Marchetti *et al.,* "Skin lesion analysis toward melanoma detection," in *Proc. Int. Symp. on Biomedical Imaging(ISBI)*, IEEE, Prague, Czech Republic, pp. 96–109, 2016.

[4]   Q. Song, L. Zhao, X. Luo and X. Dou, "Using deep learning for classification of lung nodules on computed tomography images," *Journal of Healthcare Engineering*, vol. 2017, 2017.

[5]   T. Paulraj and K. S. Chellliah, "Computer aided diagnosis of lung cancer in computed tomography scans: A review," *Current Medical Imaging*, vol. 14, no. 3, pp. 374–388, 2018.

[6]   N. Petrick, B. Sahiner, S. G. Armato, A. Bert, L. Correale *et al.,* "Evaluation of computer-aided detection and diagnosis systems," *Medical Physics*, vol. 40, no. 8, pp. 087001, 2013.

[7]   E. L. Henriksen, J. F. Carlsen, I. M. Vejborg, M. B. Nielsen and C. A. Lauridsen, "The efficacy of using computer-aided detection (CAD) for detection of breast cancer in mammography screening: A systematic review," *Acta Radiologica*, vol. 60, no. 1, pp. 13–18, 2019.

[8]   T. Manikandan, N. Bharathi, M. Sathish and V. Asokan, "Hybrid neuro-fuzzy system for prediction of lung diseases based on the observed symptom values," *Journal of Chemical and Pharmaceutical Sciences*, vol. 974, pp. 2115, 2017.

[9]   L. Caravatta, G. Macchia, G. C. Mattiucci, A. Sainato, N. L. Cernusco *et al.,* "Inter-observer variability of clinical target volume delineation in radiotherapy treatment of pancreatic cancer: A multi-institutional contouring experience," *Radiation Oncology*, vol. 9, no. 1, pp. 1–9, 2014.

[10] K. Kavin Kumar, M. Devi and S. Maheswaran, "An efficient method for brain tumor detection using texture features and SVM classifier in MR images," *Asian Pacific Journal of Cancer Prevention: APJCP*, vol. 19, no. 10, pp. 2789, 2018.

[11] M. Shanmugam, S. Nehru and S. Shanmugam, "A wearable embedded device for chronic low back patients to track lumbar spine position," *Biomedical Research*, pp. 1–12, 2018.

[12] R. Arulmurugan and H. Anandakumar, "Early detection of lung cancer using wavelet feature descriptor and feed forward back propagation neural networks classifier," in *Proc. Computational Vision and Bio Inspired Computing*, Springer, Champ, India, pp. 103–110, 2018.

[13] P. Moradi and M. Jamzad, "Detecting lung cancer lesions in CT images using 3D convolutional neural networks," in *Proc. 2019 4th Int. Conf. on Pattern Recognition and Image Analysis (IPRIA)*, IEEE, Tehran, Iran, pp. 114–118, 2019.

[14] Q. Zhang and X. Kong, "Design of automatic lung nodule detection system based on multi-scene deep learning framework," *IEEE Access*, vol. 8, pp. 90380–90389, 2020.

[15] A. Asuntha and A. Srinivasan, "Deep learning for lung cancer detection and classification," *Multimedia Tools and Applications*, vol. 79, no. 11, pp. 7731–7762, 2020.

[16] O. Ozdemir, R. L. Russell and A. A. Berlin, "A 3D probabilistic deep learning system for detection and diagnosis of lung cancer using low-dose CT scans," *IEEE Transactions on Medical Imaging*, vol. 39, no. 5, pp. 1419–1429, 2019.

[17] M. Vas and A. Dessai, "Lung cancer detection system using lung CT image processing," in *Proc. 2017 Int. Conf. on Computing, Communication, Control and Automation (ICCUBEA)*, IEEE, Pune, India, pp. 1–5, 2017.

[18] A. Teramoto, T. Tsukamoto, Y. Kiriyama and H. Fujita, "Automated classification of lung cancer types from cytological images using deep convolutional neural networks," *BioMed Research International*, vol. 2017, 2017.

[19] M. Šarić, M. Russo, M. Stella and M. Sikora, "CNN-Based method for lung cancer detection in whole slide histopathology images," in *Proc. 2019 4th Int. Conf. on Smart and Sustainable Technologies*, IEEE, Split, Croatia, pp. 1–4, 2019.

[20] M. S. Rahman, P. C. Shill and Z. Homayra, "A new method for lung nodule detection using deep neural networks for CT images," in *Int. Conf. on Electrical, Computer and Communication Engineering (ECCE)*, pp. 1–6, 2019, 2019.

[21] J. Alam, S. Alam and A. Hossan, "Multi-stage lung cancer detection and prediction using multi-class svm classifie," in *Proc. Int. Conf. on Computer, Communication, Chemical, Material and Electronic Engineering(IC4ME2)*, Rajshahi, Bangladesh, pp. 1–4, 2018.

[22] S. Shanthi and N. Rajkumar, "Lung cancer prediction using stochastic diffusion search (SDS) based feature selection and machine learning methods," *Neural Processing Letters*, vol. 53, no. 4, pp. 2617–2630, 2021.

[23] Y. Xie, Y. Xia, J. Zhang, Y. Song, D. Feng *et al.,* "Knowledge-based collaborative deep learning for benign-malignant lung nodule classification on chest CT," *IEEE Transactions on Medical Imaging*, vol. 38, no. 4, pp. 991–1004, 2018.

[24] J. Esther and M. Mohamed Sathik, "An analytical study on query integration in image retrieval system," *International Journal of Advanced Research in Computer Science*, vol. 3, no. 2, 2012.

[25] M. Sajjad, S. Khan, K. Muhammad, W. Wu, A. Ullah *et al.,* "Multi-grade brain tumor classification using deep CNN with extensive data augmentation," *Journal of Computational Science*, vol. 30, pp. 174–182, 2019.

[26] P. Surendar, "Diagnosis of lung cancer using hybrid deep neural network with adaptive sine cosine crow search algorithm," *Journal of Computational Science*, vol. 53, pp. 101374, 2021.

[27] K. Senthil Kumar, K. Venkatalakshmi and K. Karthikeyan, "Lung cancer detection using image segmentation by means of various evolutionary algorithms," *Computational and Mathematical Methods in Medicine,* vol. 2019, 2019.

[28] V. A. Devi, "Detection of novel coronavirus (nCov-2019) using lung CT scan by marker-based watershed segmentation method," *International Journal of Innovative Research in Applied Sciences and Engineering*, vol. 4, no. 5, pp. 766–780, 2020.

[29] S. Uzelaltinbulat and B. Ugur, "Lung tumor segmentation algorithm," *Procedia Computer Science*, vol. 120, pp. 140–147, 2017.

[30] M. F. Serj, B. Lavi, G. Hoff and D. P. Valls, "A deep convolutional neural network for lung cancer diagnostic," *Arxiv Preprint Arxiv:1804.08170*, 2018.

[31] B. A. Skourt, A. ElHassani and A. Majda, "Lung CT image segmentation using deep neural networks," *Procedia Computer Science*, vol. 127, pp. 109–113, 2018.

[32] S. Suresh and S. Mohan, "NROI based feature learning for automated tumor stage classification of pulmonary lung nodules using deep convolutional neural networks," *Journal of King Saud University-Computer and Information Sciences*, 2019.

[33] S. Lakshmanaprabu, S. N. Mohanty, K. Shankar, N. Arunkumar and G. Ramirez, "Optimal deep learning model for classification of lung cancer on CT images," *Future Generation Computer Systems*, vol. 92, pp. 374–382, 2019.

[34] A. O. Carvalho Filho, A. C. Silva, A. C. de Paiva, R. A. Nunes and M. Gattass, "Classification of patterns of benignity and malignancy based on CT using topology-based phylogenetic diversity index and convolutional neural network," *Pattern Recognition*, vol. 81, pp. 200–212, 2018.

[35] Y. Xie, J. Zhang, Y. Xia, M. Fulham and Y. Zhang, "Fusing texture, shape and deep model-learned information at decision level for automated classification of lung nodules on chest CT," *Information Fusion*, vol. 42, pp. 102–110, 2018.

[36] W. Shen, M. Zhou, F. Yang, C. Yang and J. Tian, "Multi-scale convolutional neural networks for lung nodule classification," in *Proc. Information Processing in Medical Imaging(IPMI)*, Sabhal Mor Ostaig, Isle of Skye, United Kingdom, pp. 588–599, 2015.